Journal of Catalysis 426 (2023) 270–282

Contents lists available at ScienceDirect

Journal of Catalysis

journal homepage: www.elsevier.com/locate/jcat

Controlling polyethylene branching via surface confinement of Ni complexes

Ruikai Wu [a,b], Tim M. Lenz [c], Lucas Stieglitz [c], Raphaël Galois [a], Ruohan Zhao [a], Patrick Rupper [a], Sandro Lehner [a], Milijana Jovic [a], Antonia Neels [d], Sabyasachi Gaan [a,*], Bernhard Rieger [c], Manfred Heuberger [a,b,*]

[a] Laboratory of Advanced Fibers, Empa, Swiss Federal Laboratories for Materials Science and Technology, Lerchenfeldstrasse 5, 9014 St. Gallen, Switzerland
[b] Department of Materials, ETH Zurich, 8092 Zurich, Switzerland
[c] WACKER-Chair of Macromolecular Chemistry, Catalysis Research Center, Technical University Munich, Lichtenbergstraße 4, 85748 Garching, Germany
[d] Center for X-ray Analytics, Empa, Swiss Federal Laboratories for Materials Science and Technology, Überlandstrasse 129, 8600 Dübendorf, Switzerland

ARTICLE INFO

Keywords:
α-Diimine Ni (II) complexes
Chain-walking process
Covalent immobilization
Supported catalyst
Slurry-phase polymerization
High molecular weight
PE microstructure

ABSTRACT

The heterogeneous surface support can play a key role in determining polymer microstructure, as we show for a novel variant of Ni-catalyst from the family of late-transition metal complexes; this extends the toolbox for novel catalytic solutions in industrial processes. Novel variants of single-atom catalysts (**Ni-FO-Al@SiO_2**, **Ni-FO-Si@SiO_2**, **Ni-O-Al@SiO_2**, and **Ni-O-Si@SiO_2**) were prepared in the form of unsymmetrical *α*-diimine Ni complexes (**Ni-OH** and **Ni-FOH**) and then characterized by inductively coupled plasma - optical emission spectrometry (ICP-OES) and X-ray photoelectron spectroscopy (XPS) analysis. Ethylene slurry-phase polymerization was performed both via self-supporting and covalent-tethering strategies to systematically study the surface confinement effects. High catalytic activity was maintained under the slurry-phase polymerization (as high as 3.9×10^6 g of PE (mol of Ni)$^{-1}$ h^{-1}). The crucial features of high molecular weight (>10^6 g mol^{-1}) and high branching density (as high as 180.1BD/1000C) were found among the PE samples produced via heterogeneous polymerization. A detailed investigation suggested that surface functional groups, such as —OH and —Cl, coordinate with the active Ni species via their lone pairs and terminate the ethylene polymerization. Microstructure analysis of the PE confirm that the supporting substrate provides the chance to modulate the chain-walking behavior of these Ni catalysts. Systematic high-temperature ^{1}H and ^{13}C NMR analysis indicated that the PE branching density could significantly decrease by surface confinement from the solid substrate. Until now, such microstructure control has been mainly realized via the laborious synthesis of bulky *α*-diimine ligands.

1. Introduction

Currently, late-transition metal complexes are emerging as a potential alternative to present-day olefin catalysts in the industry [1]. The single-site catalytic centers of these late-transition metals enable the synthesis of polymers with a narrow molecular weight distribution. Microstructures and macromolecular characteristics of the tailored polymers are commonly modulated by a variation of the ligand structure and metal center [2]. In addition, the low-oxophilic nature of late-transition complexes facilitates an ethylene copolymerization with polar monomers [3,4]. The incorporation of the functional groups in the polymer chains has significantly increased their potential industrial exploitation. Among the late-transition metal complexes, the α-diimine Ni and Pd complexes are the most well-studied olefin catalysts for ethylene (co)polymerization and feature an easy synthesis and air/moisture stability [5–8]. Besides their advantage in the copolymerization with polar monomers, the structural modifications on *N*-aryl, backbone, and remote substituent effects have been considered as key variables, influencing the catalytic behavior of α-diimine Ni complexes via a so-called chain-walking mechanism: the catalytic Ni^+ migrates along the polyethylene backbone via rapid *β*-H elimination and reinsertion as a chain-walking process. The PE M_W depends on the competition between the monomer insertion (chain growth) and the *β*-H elimination (chain transfer) processes. The latter, when followed by the reinsertion, is understood to lead to the formation of branched structures. Therefore, thermoplastic elastomers can be easily synthesized

* Corresponding authors.
E-mail addresses: sabyasachi.gaan@empa.ch (S. Gaan), manfred.heuberger@empa.ch (M. Heuberger).

https://doi.org/10.1016/j.jcat.2023.07.019
Received 7 June 2023; Received in revised form 19 July 2023; Accepted 20 July 2023
Available online 22 July 2023

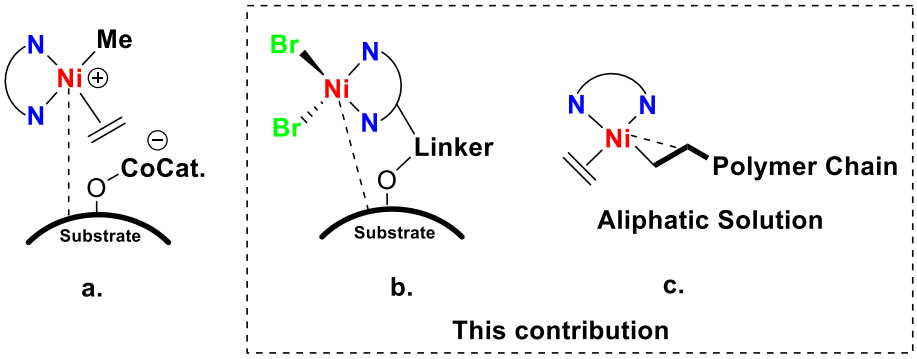

Fig. 1. Supported α-diimine Ni complexes for ethylene heterogeneous polymerization.

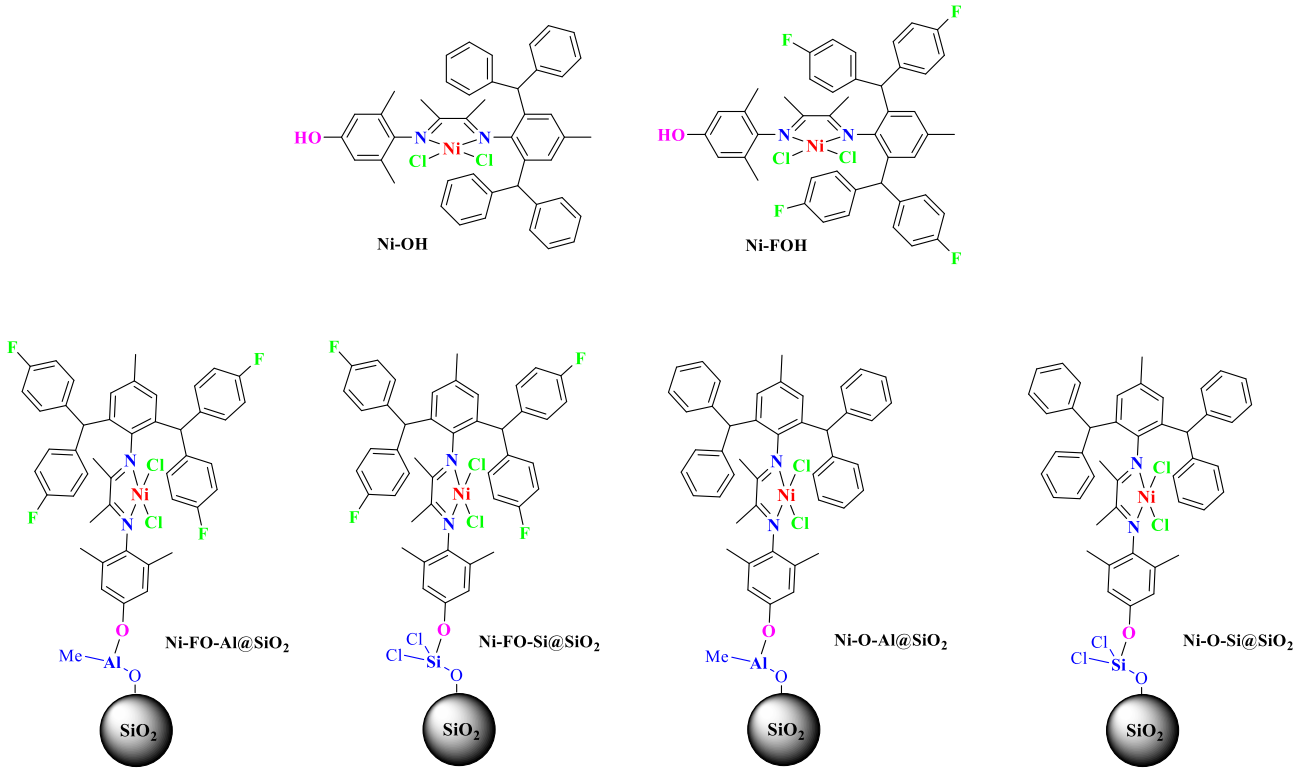

Fig. 2. Illustration of α-diimine Ni complexes and surface-tethered SACs used in this work.

through this controlled chain-walking process [9–14], where only ethylene serves as a reactive monomer [15]. Most efforts in controlling the PE branching and molecular weight have focused primarily on ligands design. Bulky ligands slow the chain walking process and reduce the branching density. An effect of surface immobilization of Ni complexes on PE branching has been mentioned earlier, however, a systematic study of this interesting influence is missing [2,16].

In the field of homogeneous polymerization, the catalytic behavior of the α-diimine Ni complexes is mainly altered by the structural modifications and polymerization conditions [17–19]. Currently, plenty of research works are related to newly designed α-diimine Ni complexes focusing on homogeneous systems, which can be considered as the well-established platform for further commercial application. However, the synthesis of polyolefins in industry is mainly dominated by heterogeneous polymerizations, especially for Ziegler-Natta and Phillips catalysts [20,21]. Supported α-diimine Ni complexes in ethylene heterogeneous polymerization have not yet attracted much attention in neither academia nor industry. In addition, the multi-site catalytic mechanism, which has been commercially applied in industry, is poorly understood [22]. The successful utilization of heterogeneous single-atom catalysts (SACs) will definitely bridge the present academic research and future application based on α-diimine Ni complexes [23]. Up to now, researchers have focused on the gas- and slurry-phase polymerization catalyzed by the α-diimine Ni complexes. Generally, the supporting methods can be classified according to their immobilization techniques: surface-bound anions (**a.** in Fig. 1) and covalent attachment (**b.** in Fig. 1) [2,16,23–28]. The former approach involves the pretreatment of the inorganic supports with a cocatalyst to generate surface-bound Al compounds (CoCat. In Fig. 1.). Subsequently, the Al compounds serve as the initiator to convert the α-diimine Ni complexes into the catalytic active species and simultaneously bind them to the solid surface. The second method involves the covalent bonding between the solid supports and α-diimine Ni complexes, with the aid of a functional linker. More recently, a self-supporting strategy (**c.** in Fig. 1) has been explored for ethylene polymerization. Thanks to the chain-walking behavior of α-diimine Ni complexes, the active site covalently connects and migrates along the polymer chains. In the nonpolar aliphatic solution, the polymer chain produced from the polymerization could also serve as the

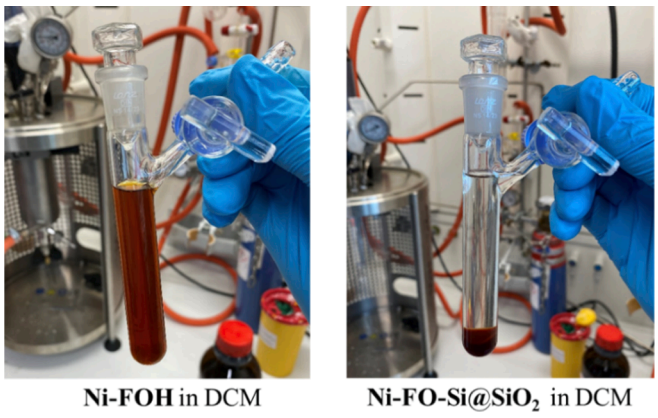

Fig. 3. Graphic illustration of the difference between the soluble **Ni-FOH** and covalent immobilized SACs (**Ni-FO-Si@SiO_2**).

insoluble support for the active sites [29].

Studies on heterogeneous polymerization using α-diimine Ni complexes still remain in their infancy [2]. The control over PE microstructures using such heterogenization of Ni complexes is worth investigating. Bulky ligands in combination with the solid substrate significantly influence the chain-walking behavior of differently surface-tethered α-diimine Ni complexes. In this work, two different α-diimine Ni complexes (**Ni-OH** and **Ni-FOH**) were synthesized, well-characterized, and subsequently anchored on silica particles for ethylene slurry-phase polymerization (Fig. 2). The incorporation of the hydroxyl group at the *para*-N-aryl allows covalent tethering of the α-diimine Ni complexes onto the SiO_2 particles. The resulting heterogeneous SACs (**Ni-FO-Al@SiO_2**, **Ni-FO-Si@SiO_2**, **Ni-O-Al@SiO_2**, and **Ni-O-Si@SiO_2** in Fig. 2) open pathways to systematically investigate the different catalytic behaviors in ethylene polymerization, comparing to the current catalysts applied in the industry. Meanwhile, understanding the difference in the catalytic performance between heterogeneous and homogeneous ethylene polymerization will help develop an optimized polymerization process. The solid support has a similar confining effect as the steric volume of a ligand, thus providing unique coordination environments to active Ni sites among the ethylene monomer insertion. The chain-growth and chain-transfer process under the ethylene slurry-phase polymerization will be retarded for heterogeneous SACs. Hydrogen reinsertion leads to a chain-walking process, which produces various branching densities of the synthesized PE. The substrate surface possibly exhibits toxic functional groups, which might terminate the chain-growth/walking polymerization. It is expected that the catalytic activity of the heterogeneous SACs and the microstructures (such as branches, M_w, PDI, and melting transition) of the produced PE should be different as compared to homogenous polymerization. The self-supporting and covalent-tethering strategies utilized in this work provide a platform to gain additional insights into the surface-confinement effects of Ni-catalyzed ethylene polymerization.

2. Result and discussion

2.1. *Synthesis of α-diimine Ni complexes and heterogeneous SACs*

The synthesis of the **Ni-OH** and **Ni-FOH** mainly involved the complexation reaction from the $NiCl_2{\cdot}6H_2O$ and **L-OH**/**L-FOH**, which were generated from the corresponding imine formation reactions (Fig. 3) [15,30]. The α-diimine Ni complexes (**Ni-OH** and **Ni-FOH**) were characterized by elemental analysis, high-resolution electrospray ionization mass spectrometry, and single-crystal X-ray diffraction (Figs. S1 and S2). The preparation of the heterogeneous SACs (**Ni-FO-Al@SiO_2**, **Ni-FO-Si@SiO_2**, **Ni-O-Al@SiO_2**, and **Ni-O-Si@SiO_2**) was primarily carried out with the chemisorption method reported by *Brookhart et al.* α-Diimine nickel(II) complexes with a hydroxyl functionality reacted with trimethylaluminum (TMA) or silicon (IV) chloride ($SiCl_4$)-treated silica to generate the covalently linked catalysts [23,25]. In contrast to previous studies, an unsymmetrical synthetic strategy was applied to incorporate a single hydroxyl group on the *para*-*N*-aryl of the α-diimine Ni complexes. Meanwhile, the bulky *ortho*-*N*-aryl groups with various dibenzhydryl substitutions were also combined with the heterogeneous SACs (Scheme 1). With this strategy, we aim at altering the chain-walking behaviors and the molecular weights of the produced PE in the slurry-phase polymerization. The terminal hydroxyl group was used for surface-tethering, presumably leading to a preferential surface orientation. During the immobilization process of the SACs, one equivalent HCl or CH_4 was generated and released as the byproduct [25]. The metal loading concentration of the heterogeneous SACs was determined by the ICP-OES analysis. It is worth noting that the amount of Ni content among the produced heterogeneous SACs is relatively different. This interesting observation can be possibly attributed to the structural features (electronic and steric effects) of the Ni complexes and different interactions with the applied linkers. In addition, the Al loading concentration in **Ni-FO-Al@SiO_2** and **Ni-O-Al@SiO_2** is much higher than the Ni loading. It also explains the great possibility of the complete reaction between $AlMe_3$ and Si-OH from silica substrate and the formation of the $(Si\text{-}O)_3\text{-}Al$ during the functionalization of the supporting substrate.

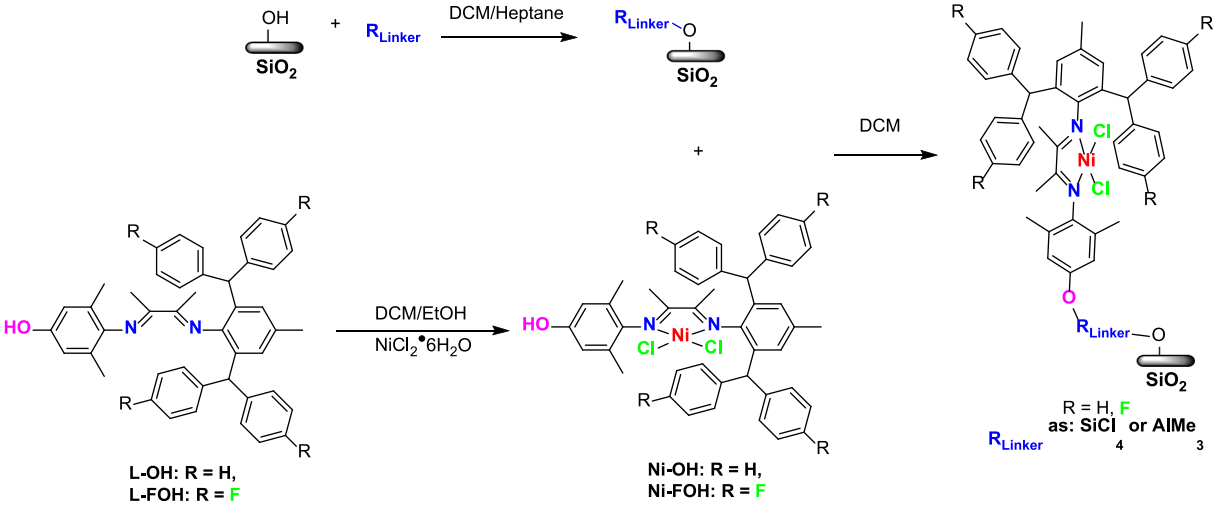

Scheme 1. Synthesis of α-diimine Ni complexes/ heterogeneous SACs for ethylene slurry-phase polymerization.

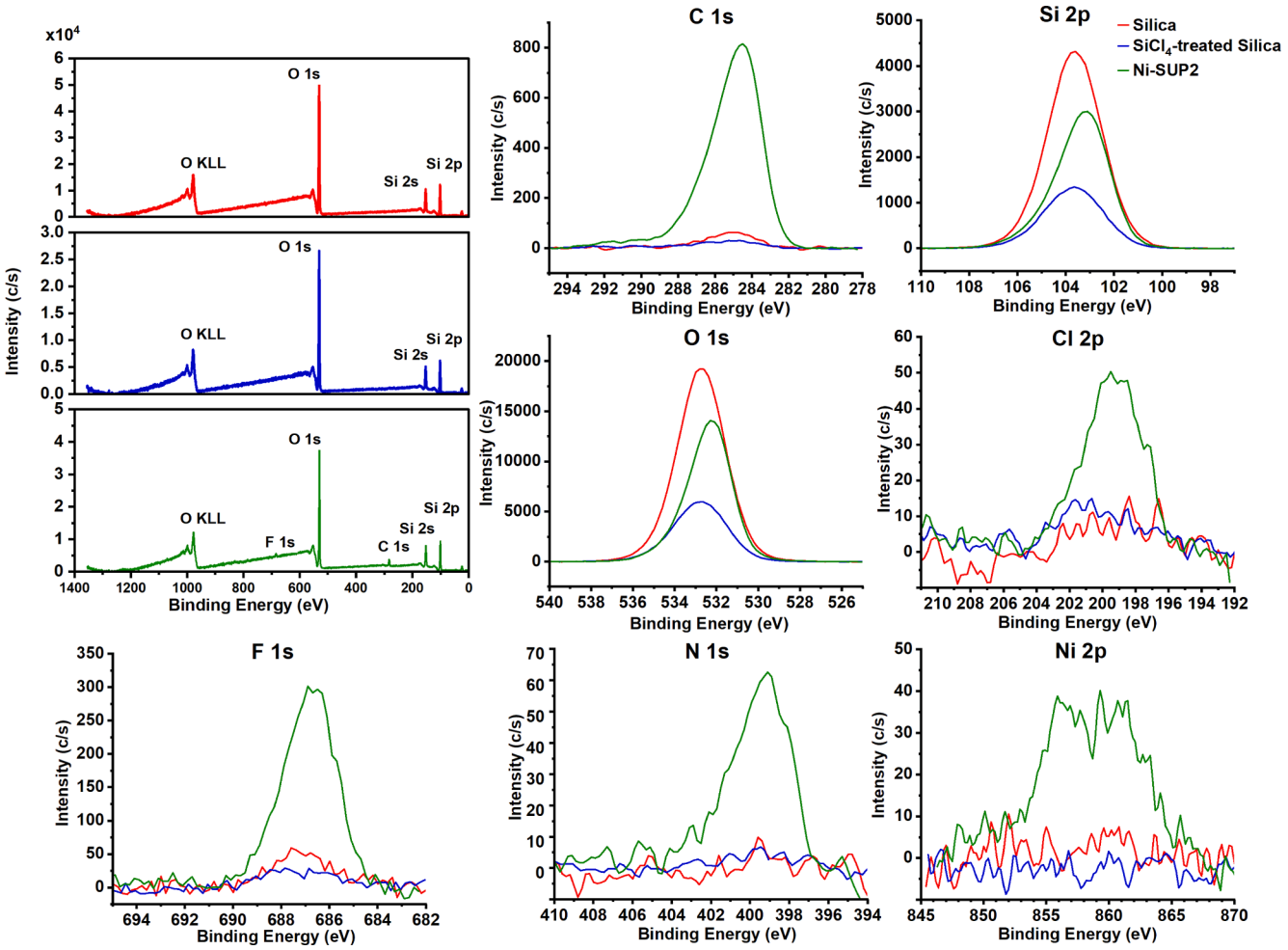

Fig. 4. XPS surface characterization of initial silica, $SiCl_4$-treated silica, and **Ni-FO-Si@SiO$_2$**, where the survey scan and detail scans of C 1 s, Si 2p, O 1 s, Cl 2p, Ni 2p, N 1 s and F 1 s are presented individually. The apparently negative values shown in Cl 2p, Ni 2p, and N 1 s are an inevitable graphical artifact due to noise affecting background subtraction.

Table 1
Ethylene slurry-phase polymerization with self-supported Ni precatalysts.[a]

Entry	Ni	CoCat.	T, ° C	t, min	Yield, g	Act.[b]	M_w[c]	M_w/M_n[c]	T_m[d], ° C
1	**Ni-FOH**	Me_2AlCl	0	60	0.05	0.01	0.70	3.4	125.4
2	**Ni-FOH**	Me_2AlCl	20	60	1.04	0.21	0.73	3.9	121.4
3	**Ni-FOH**	Me_2AlCl	30	60	3.88	0.78	1.10	2.5	92.3
4	**Ni-FOH**	Me_2AlCl	40	60	7.68	1.54	0.77	2.6	82.8
5	**Ni-FOH**	Me_2AlCl	60	60	7.17	1.43	0.50	2.4	–
6	**Ni-FOH**	Me_2AlCl	80	60	4.36	0.87	0.21	2.3	–
7	**Ni-FOH**	EASC	0	60	0.20	0.04	0.76	3.4	124.2
8	**Ni-FOH**	EASC	20	60	0.70	0.14	0.80	3.3	120.1
9	**Ni-FOH**	EASC	30	60	3.33	0.67	1.64	2.4	93.1
10	**Ni-FOH**	EASC	40	60	9.10	1.82	0.80	2.5	86.3
11	**Ni-FOH**	EASC	60	60	7.90	1.58	0.42	2.3	–
12	**Ni-FOH**	EASC	80	60	5.65	1.13	0.21	2.4	–
13	**Ni-OH**	EASC	40	60	19.52	3.90	1.01	2.5	90.5
14	**Ni-OH**	EASC	60	60	13.74	2.75	0.45	2.7	–
15	**Ni-OH**	EASC	80	60	6.99	1.40	0.26	2.3	–

[a] General conditions: 5 μmol of **Ni** precatalysts; Al/Ni = 500; 10 bar of ethylene gas (constant flow); 100 mL total volume of anhydrous heptane; 3000 r/min.
[b] Unit of 10^6 g of PE (mol of Ni)$^{-1}$ h^{-1}.
[c] Unit of 10^6 g mol^{-1}, determined by GPC in 1,2,4-trichlorobenzene at 160 °C versus linear polystyrene standards.
[d] Determined by DSC (second heating scan).

As shown in Fig. 3, the dichloromethane solutions of α-diimine Ni complex (**Ni-FOH**) and heterogeneous SACs (**Ni-FO-Si@SiO2**) were significantly different in brown color, indicating colorless solvent with **Ni-FO-Si@SiO2,** i.e. after immobilization. In contrast to **Ni-FOH,** which is fully soluble in DCM, **Ni-FO-Si@SiO$_2$** completely precipitates in DCM, leaving behind a completely clear and colorless supernatant and a colored sediment at the bottom of the glass tube. This finding suggests a complete covalent attachment to the solid support, since physisorbed

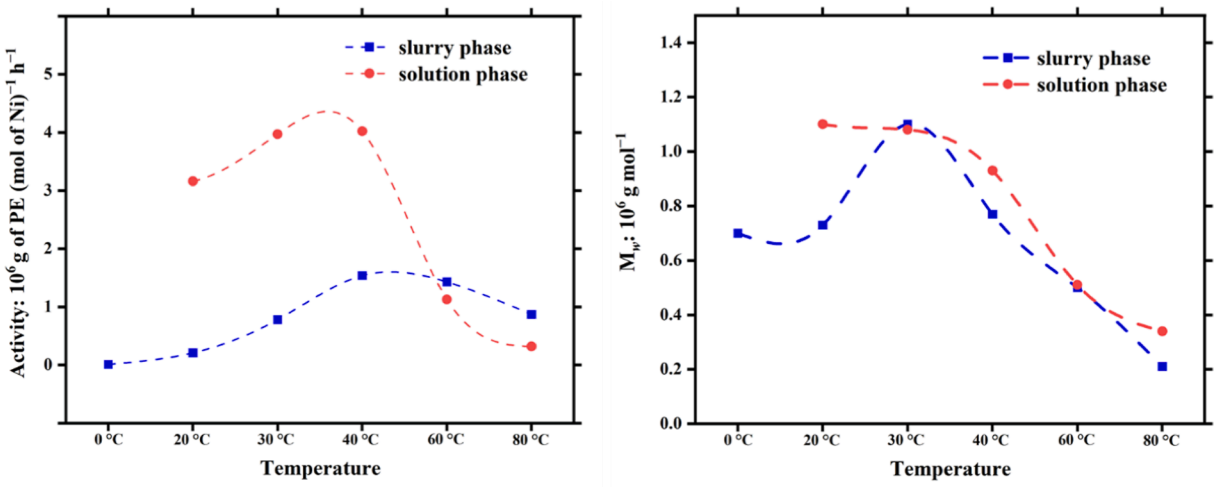

Fig. 5. Comparison of the catalytic activity and M_w between the slurry-phase and solution-phase polymerization catalyzed by **Ni-FOH**/Me_2AlCl.

Table 2
Ethylene slurry-phase polymerization with covalently supported Ni precatalysts.[a]

Entry	Ni	CoCat.	T, ° C	t, min	Yield, g	Act.[b]	M_w[c]	M_w/M_n[c]	T_m[d], ° C
1	**Ni-FO-Al@SiO$_2$**	EASC	20	60	0.86	1.72	1.15	2.6	122.4
2	**Ni-FO-Al@SiO$_2$**	EASC	40	60	0.93	1.86	1.01	6.9	120.4
3	**Ni-FO-Al@SiO$_2$**	EASC	60	60	0.73	1.46	0.60	2.8	119.4
4	**Ni-FO-Al@SiO$_2$**	EASC	80	60	0.29	0.58	0.53	2.5	119.1
5	**Ni-O-Al@SiO$_2$**	EASC	20	60	0.34	0.68	0.77	3.7	125.6
6	**Ni-O-Al@SiO$_2$**	EASC	40	60	1.12	2.24	0.54	5.4	121.4
7	**Ni-O-Al@SiO$_2$**	EASC	60	60	1.15	2.30	0.57	3.6	119.0
8	**Ni-O-Al@SiO$_2$**	EASC	80	60	0.54	1.08	0.31	4.4	119.6
9	**Ni-O-Al@SiO$_2$**	EASC	40	120	1.87	1.87	1.10	6.0	121.0
10[e]	**Ni-O-Al@SiO$_2$**	EASC	40	60	0.51	1.02	0.93	5.3	119.8
11	**Ni-FO-Si@SiO$_2$**	EASC	40	60	0.16	0.32	0.91	6.0	118.4
12	**Ni-O-Si@SiO$_2$**	EASC	40	60	0.21	0.42	0.72	4.9	118.6

[a] General conditions: 5 μmol (theoretical) of **Ni** precatalysts; Al/Ni = 500; 100 mL total volume of anhydrous toluene; 10 bar of ethylene gas (constant flow); 3000 r/min.
[b] Unit of 10^5 g of PE (mol of Ni)$^{-1}$ h^{-1}.
[c] Unit of 10^6 g mol^{-1}, determined by GPC in 1,2,4-trichlorobenzene at 160 °C versus linear polystyrene standards.
[d] Determined by DSC (second heating scan).
[e] 5 μmol (theoretical) of **Ni** precatalysts; Al/Ni = 500; 100 mL total volume of anhydrous heptane; 10 bar of ethylene gas (constant flow); 3000 r/min.

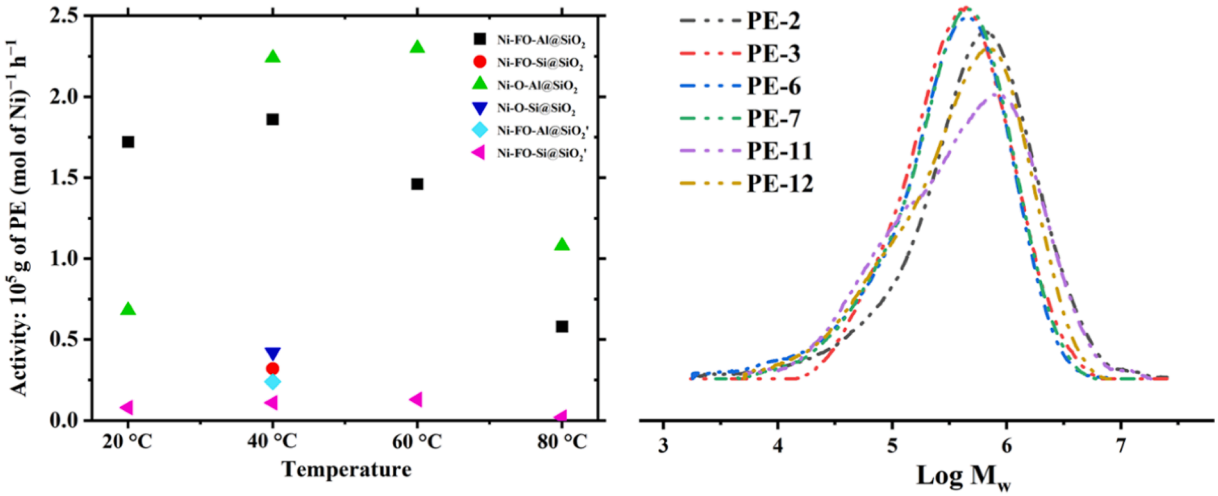

Fig. 6. Plots of the catalytic activity of Silica surface tethered Ni complexes (left) and GPC traces (right) of the selected PE samples are also shown in Table 2.

Ni-FOH would have leached out and colored the solution at equilibrium. Furthermore, X-ray photoelectron spectroscopy (XPS) was used to confirm the covalent surface attachment of the metal complex to the solid support. For these measurements, silica, silicon (IV) chloride ($SiCl_4$)-treated silica, and surface with **Ni-FO-Si@SiO$_2$** decoration were used. The surface elemental analysis is shown in Fig. 4. For silica and

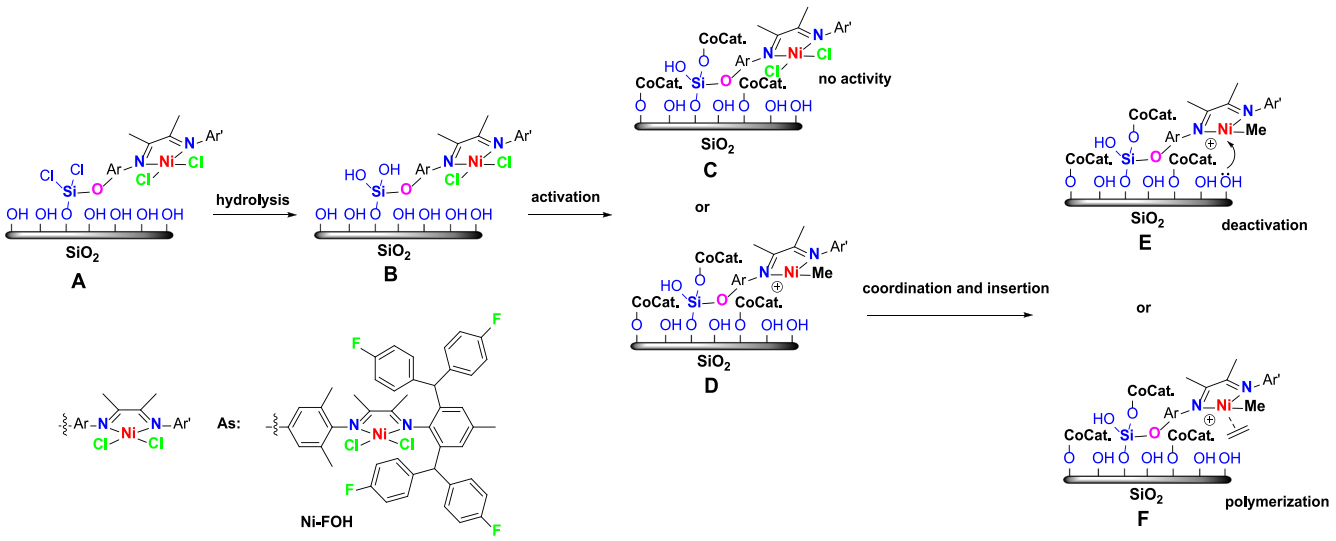

Fig. 7. Proposed deactivation mechanism on ethylene polymerization catalyzed by silica-supported **Ni-FOH** (**Ni-FO-Si@SiO$_2$**′).

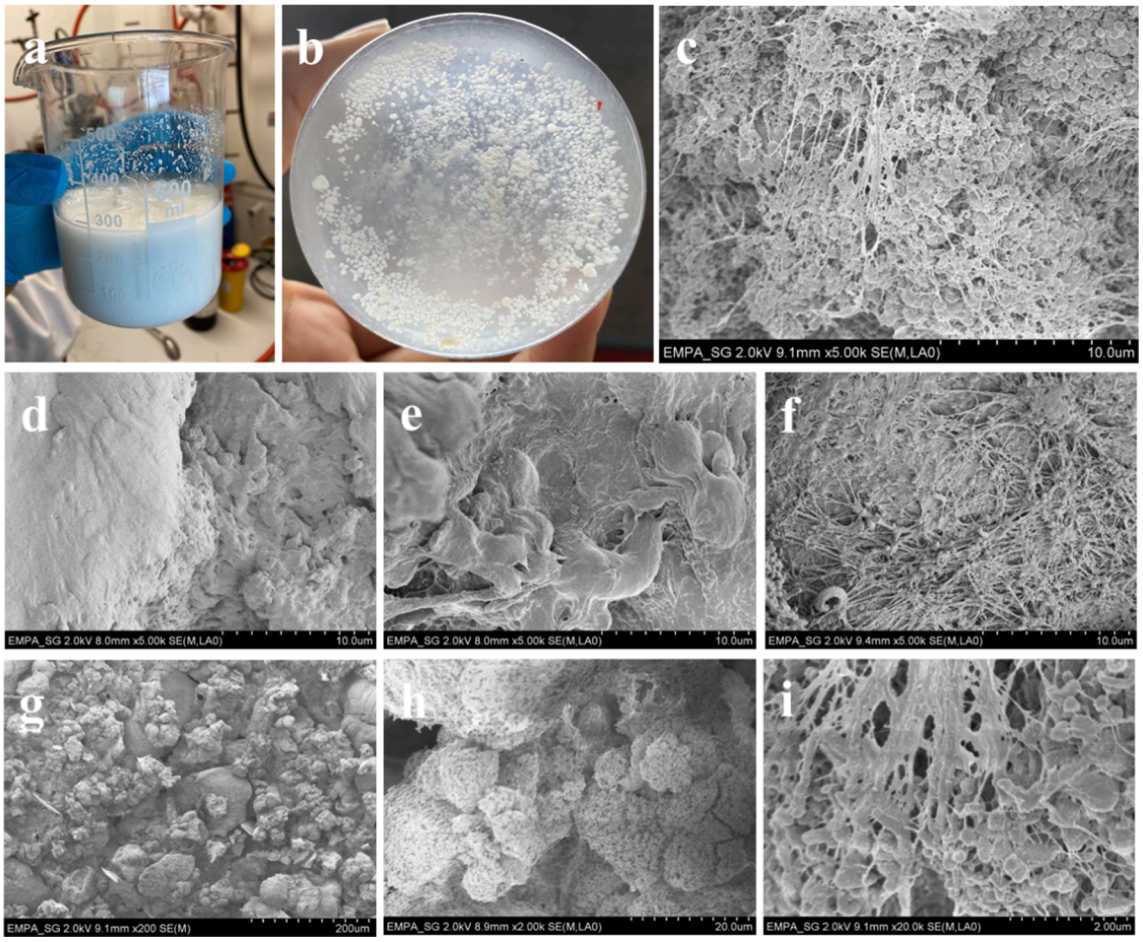

Fig. 8. Photographic and SEM pictures of PE samples synthesized via catalyzed ethylene polymerization. (a) PE samples obtained using Ni-OH in heptane (Entry 13, Table2); (b) PE samples obtained using Ni-FO-Si@SiO$_2$′ in toluene (Entry 2, Table S3); (c) SEM image of PE obtained using Ni-O-Al@SiO$_2$ in heptane (Entry 10, Table 2); (d) SEM image of PE obtained using Ni-FOH in toluene (Entry 3, Table S1); (e) SEM image of PE obtained using Ni-FOH in heptane (Entry 10, Table 1); (f) SEM image of PE obtained using Ni-O-Al@SiO$_2$ in toluene (Entry 6, Table 2); (g) reduced magnification of image (c); (h) reduced magnification of image (c); (i) enlarged magnification of image (c).

$SiCl_4$-treated silica, C 1 s peak binding energy was referenced to 285.0 eV, which corresponds to the known binding energy of the carbonaceous contamination from the air. For the silica-supported **Ni-FO-Si@SiO$_2$** sample, C 1 s peak binding energy was shifted to 284.5 eV since most of the carbon signal arises from the phenyl groups of the complex structure [31,32]. The survey scan exhibits only silicon and oxygen in significant

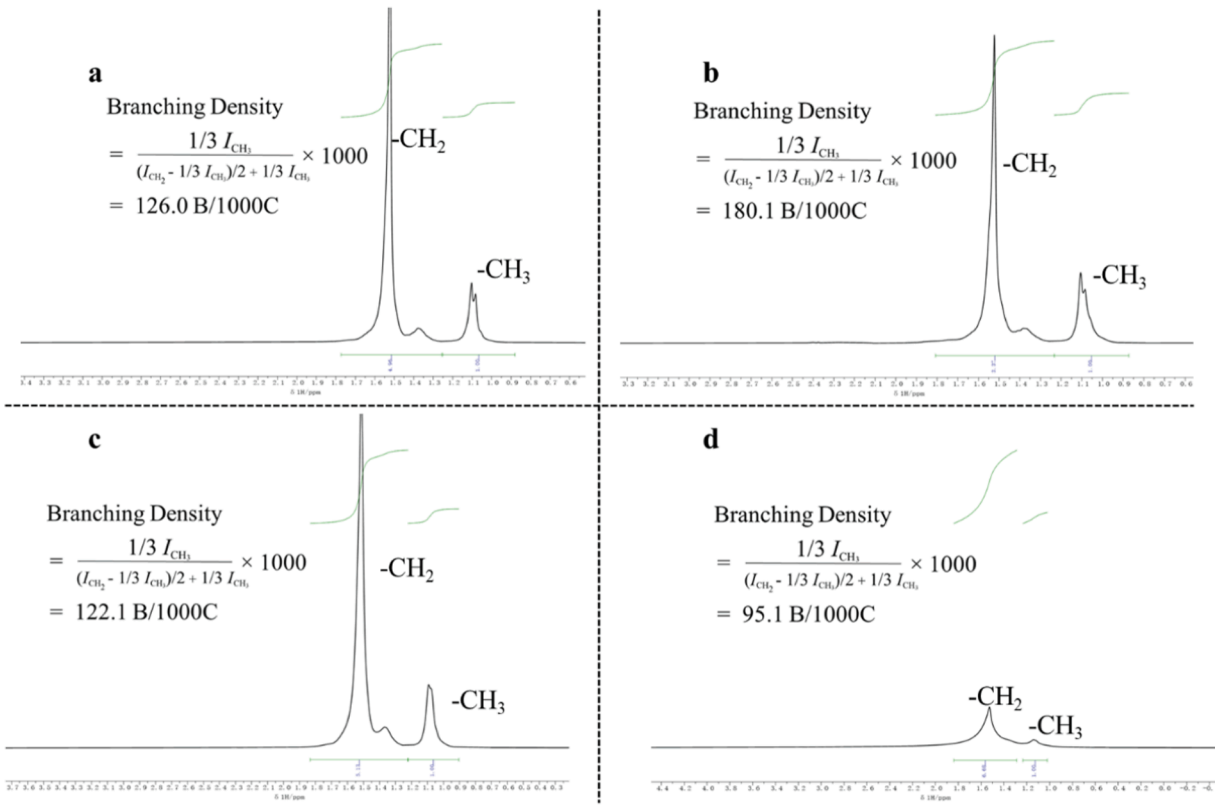

Fig. 9. High-temperature ^{1}H NMR and branching density calculation of PE samples synthesized (in Bromobenzene-d_5 at 140 °C) via catalyzed ethylene polymerization (a) PE sample in Entry 6, Table 1; (b) PE sample in Entry 12, Table 1; (c) PE sample in Entry 15, Table 1; (d) PE sample in Entry 8, Table 2.

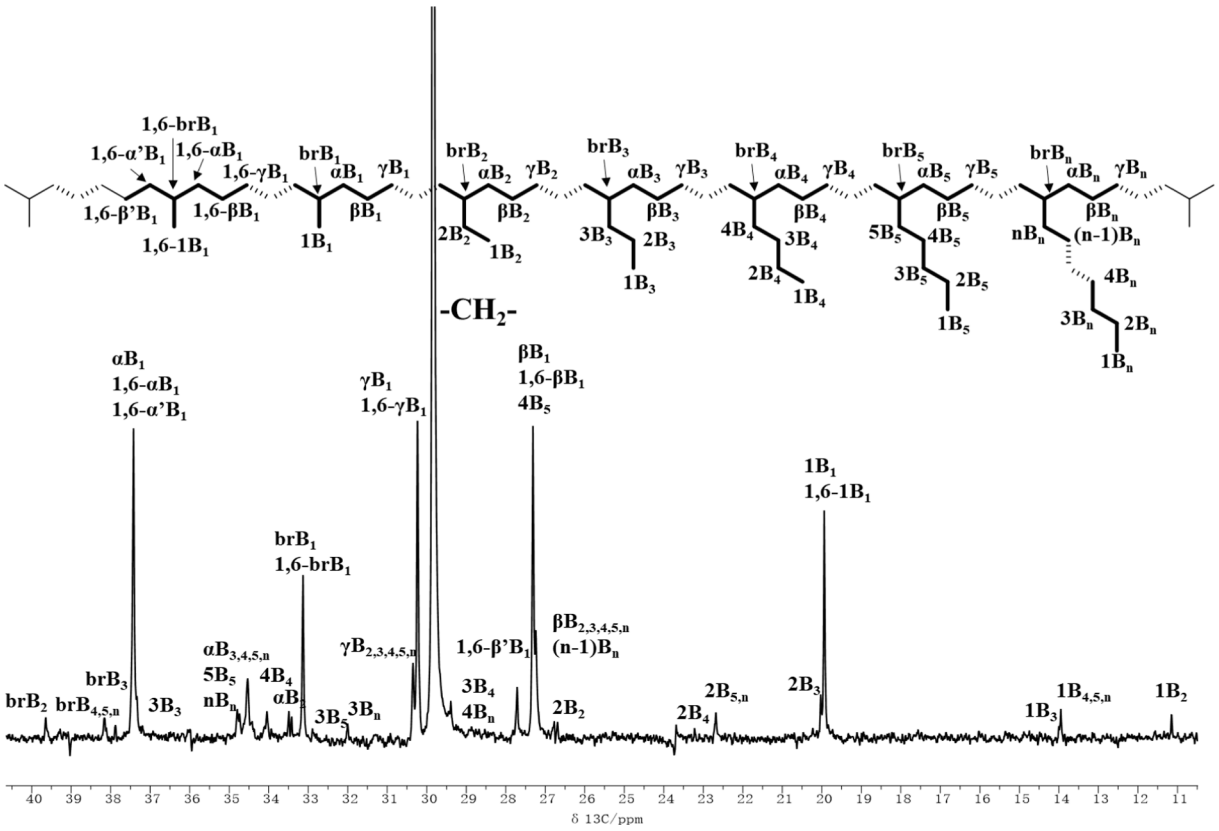

Fig. 10. High-temperature ^{13}C NMR spectra of PE sample (Entry 3, Table S1) in Bromobenzene-d_5.

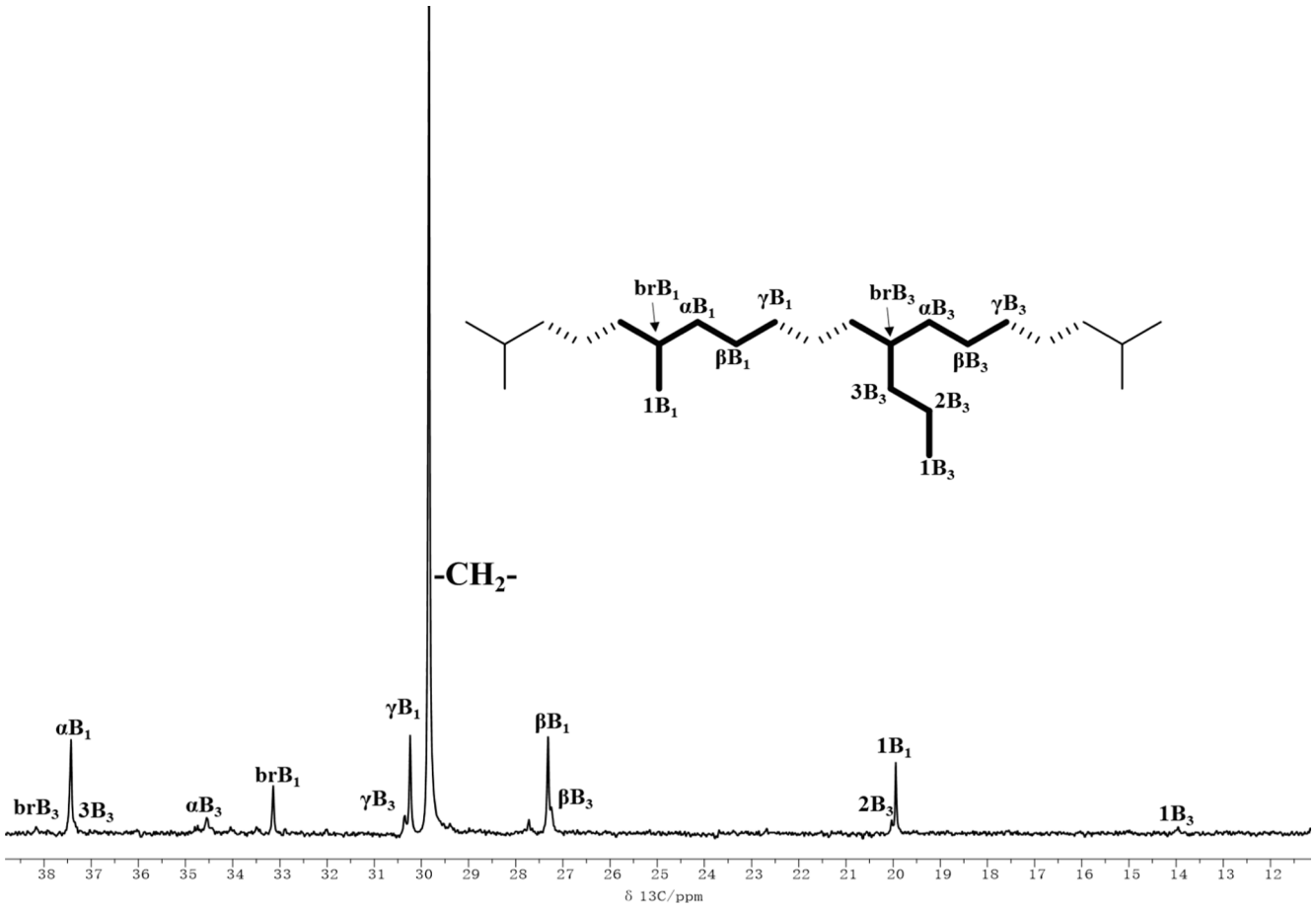

Fig. 11. High-temperature ^{13}C NMR spectra of PE sample (Entry 4, Table 1) in Bromobenzene-d_5 at 140 °C.

amounts on initial silica and $SiCl_4$-treated silica particles. For the sample **Ni-FO-Si@SiO$_2$**, the survey scan spectrum shows an additional significant carbon signal and a weak fluorine signal, which both result from successful adsorption between the tethered Ni catalyst (**Ni-FOH**) and the $SiCl_4$-treated silica substrate. The N 1 s, Ni 2p, and Cl 2p are not seen in the survey scans based on the chosen scale in the survey scan. Detailed XPS scans allowed the evaluation of further minor elements present as well as chemical state changes of the adsorbed elements in the top 2–5 nm surface region. First, nitrogen and nickel have also been found in the **Ni-FO-Si@SiO$_2$** sample, whereas they are not present in the silica samples, further confirming the presence of the specific catalyst elements on the particles. Second, for silica and $SiCl_4$-treated silica particles, there is only a trace amount of chlorine present on the surface. The hydrolysis reaction between Si-Cl and moisture from the air effectively converts Si-Cl to Si-OH groups with subsequent removal of HCl during rinsing and introduction to the vacuum chamber. In contrast, a significant amount of chlorine is observed for the **Ni-FO-Si@SiO$_2$** surface, which is linked to the Ni centers. The additional Cl signal thus confirms the presence of chlorine and thus also the efficient protection of the bulky N-aryls around the Ni center from direct interaction with a functionalized solid substrate. The covalent immobilization can be seen as a chemical state shift of Si 2p and O 1 s; namely, a shift of about 0.3 eV towards lower binding energy was observed for **Ni-FO-Si@SiO$_2$** compared to silica and $SiCl_4$-treated silica. Because the **Ni-FO-Si@SiO$_2$** sample was thoroughly washed in order to remove any potentially physisorbed catalyst molecules, this small oxidation state shift can be attributed to the covalent bond of the **Ni-FOH** to the silica substrate.

2.2. *Self-supporting strategy for ethylene polymerization*

As mentioned above, *α*-diimine Ni complexes have been extensively studied due to their ability to generate controllable PE microstructures via the chain-walking mechanism [13,33]. The active metal center migrates along the polymer chain during the ethylene monomer insertion. This catalytic feature holds promise to work well in a self-supporting strategy for ethylene slurry-phase polymerization. Owing to the insolubility of PE in aliphatic solvents, such as heptane, the polymer chain can directly serve as a solid support for the active center, which does then not require any other substrate [29]. This strategy is expected to be successful in slurry-phase polymerization while maintaining a robust catalytic performance in comparison to solution-phase polymerization. Therefore, **Ni-OH** and **Ni-FOH** were investigated as self-supporting precatalysts for the slurry-phase polymerization in heptane solution (Table 1 and S2). Meanwhile, the solution-phase polymerization was also carried out under similar reaction conditions as a benchmark for comparison (Table S1).

According to previous work, the fluorinated Ni complexes exhibit better catalytic activity than the non-fluorinated equivalents [2]. Therefore, **Ni-FOH** (5 μmol) was selected as the precatalyst for the initial screening of ethylene slurry-phase polymerization. As previously reported, the catalytic behavior of α-diimine Ni and Pd complexes is sensitive to the reaction temperature [34]. The polymerization trials were thus performed with the Al/Ni molar ratio set constant at 500 at different temperatures to determine the catalytic activity and examine the thermal stability of the **Ni-FOH**/Me_2AlCl catalytic system (entries 1–6, Table 1). Compared to the solution-phase polymerization (Table S1), the **Ni-FOH**/Me_2AlCl exhibited significantly lower catalytic activity at 0 and 20 °C (Fig. 5). Unlike homogeneous polymerization, **Ni-**

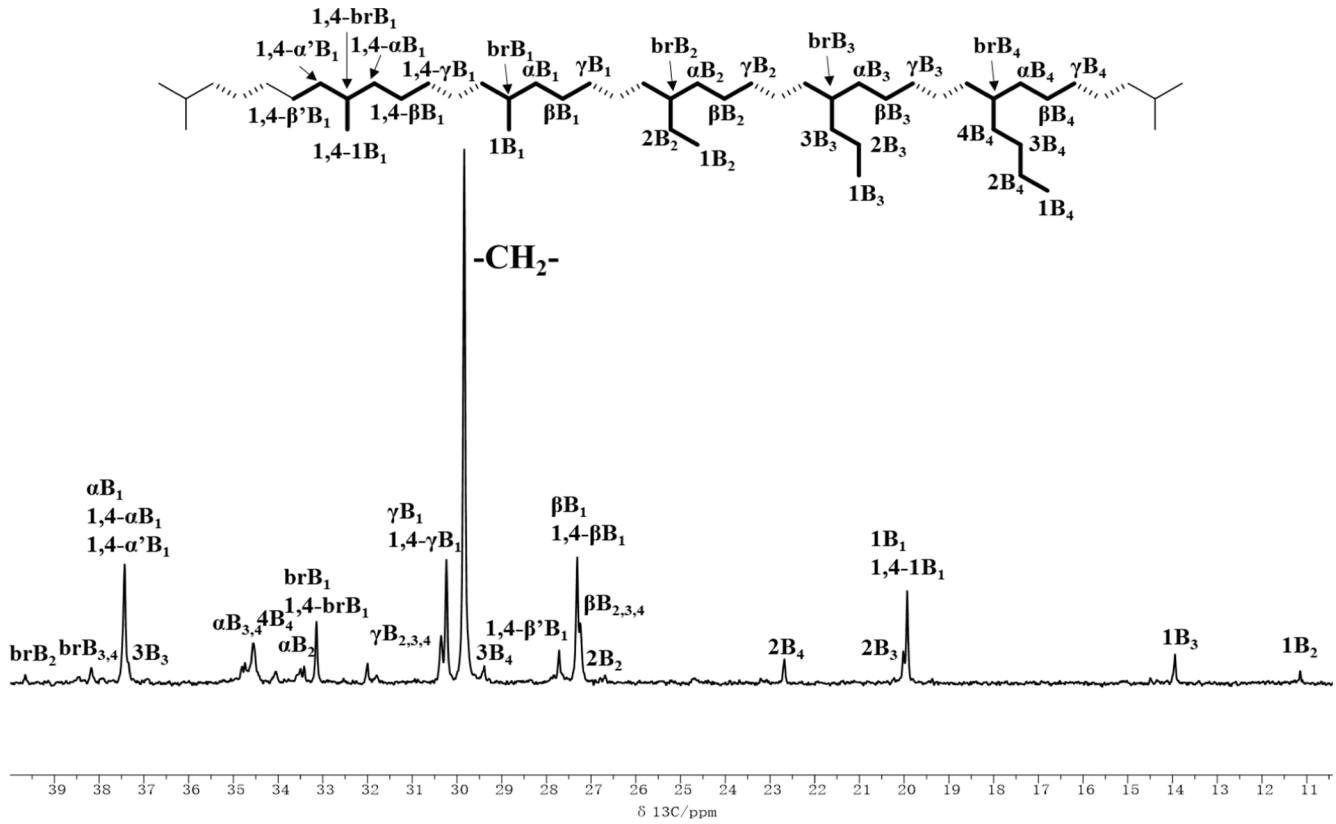

Fig. 12. High-temperature ^{13}C NMR spectra of PE sample (Entry 15, Table 1) in Bromobenzene-d_5 at 140 °C.

FOH/Me_2AlCl was not able to efficiently carry out the ethylene polymerization and polymers with a low M_w and broad PDI (3.4 and 3.4), were obtained. Similar results were observed in **Ni-FOH**/EASC (entries 7 and 8, Table 1) and **Ni-FOH**/ Et_2AlCl catalytic systems (entries 1 and 2, Table S2). As observed in Fig. 5, **Ni-FOH** exhibited higher thermal stability in heptane than in toluene. A sharp drop in the catalytic activity in solution-phase polymerization was observed above 40 °C (entries 3–5, Table S1), while relatively high catalytic activity was maintained at 40 °C in the slurry-phase polymerization (entries 4–6 and 10–12, Table 1). It can be hypothesized that the solution-phase polymerization can accelerate the thermal damage of the **Ni-FOH** precatalyst in comparison to the slurry phase. At 60 °C and 80 °C, the catalytic activity of the slurry-phase polymerization outperformed the activity of the homogeneous polymerization. The M_w produced from both slurry-phase and solution-phase polymerization can be considered as ultrahigh molecular weight (10^6 g mol^{-1}) at 30 °C (Fig. 5). Due to the acceleration of the chain-transfer and chain-walking process at high temperatures, the M_w steadily decreased with increasing temperature (Fig. 5). With the activation of EASC in the slurry phase, the catalytic activity of **Ni-FOH** reached a maximum [1.82 × 10^6 g of PE (mol of Ni)$^{-1}$ h^{-1}] at 40 °C, while the highest PE M_w (1.64 × 10^6 g mol^{-1}) was achieved at 30 °C. Additionally, a variation of the polymerization time was used to estimate the lifetime of the activated Ni species (entries 11 in Table 1 and 10-13 in Table S2). The highest activity [2.16 × 10^6 g (PE) mol^{-1} (Ni) h^{-1}] achieved was measured around 15 min after the beginning of the initiation, while the catalytic activity then gradually decreased from 15 min to 180 min, eventually reaching 1.02 × 10^6 g (PE) mol^{-1} (Ni) h^{-1}. However, the robust Ni complexes were still capable of performing the ethylene polymerization at a high level of catalytic activity even after 3 h of operation. According to previous studies, the "F effect" promotes chain-straightening and improves the catalytic efficiency of the initiated Ni species [35,36]. However, an interesting reverse phenomenon was observed in our study: **Ni-OH**/EASC exhibited even higher catalytic activity than **Ni-FOH**/EASC for ethylene slurry-phase polymerization in heptane (entries 13–15, Table 1); a similar trend was also observed in the molecular weight of the produced PE. This observation can be discussed in terms of a "solubility argument" as follows [37]. The C-F bond on the N-aryls increases the polarity of **Ni-FOH** compared to **Ni-OH** containing the C–H bond. As a consequence, **Ni-OH** exhibited a better dispersion in heptane and thus more efficient catalytic performance was observed for the **Ni-OH** /EASC system.

2.3. *Covalent-tethering strategy for ethylene polymerization*

The coordination-insertion polymerization catalyzed by the transition metal complexes is the main solution for polyethylene synthesis in both academia and industry [4]. Compared to homogeneous catalysis, the industry often prefers heterogeneous systems (especially for Ziegler-Natta and Phillips catalysts). This is mainly due to their superior performance in PE morphology control and avoidance of reactor fouling. The covalent-tethering strategy involves the direct immobilization of the *α*-diimine Ni complexes on SiO_2. The hence supported catalysts play a role as a single catalytic center on the substrate surface, suppressing leaching out from the substrate [38]. As shown in Table 2, the here used heterogeneous SACs were employed in ethylene polymerization under a range of conditions. Compared to homogeneous polymerization, a variation in temperature had a similar influence on the catalytic behaviors of the Ni species and PE molecular weights (Entries 1–8, Table 2). The best catalytic activity observed was as high as 2.3 × 10^5 g of PE (mol of Ni)$^{-1}$ h^{-1}, while high molecular weight PE (up to 1.15 × 10^6 g mol^{-1}) could be generated. The PE molecular weight could be increased by an extension of the polymerization time (Entry 9, Table 2). Meanwhile, moderately high catalytic activity was observed (1.87 × 10^5 g of PE (mol of Ni)$^{-1}$ h^{-1}) in 2 h polymerization. The polymerization solvent and notably also the tethering linker exerted a significant impact on the catalytic activity of the supported Ni species (Entries 10–12,

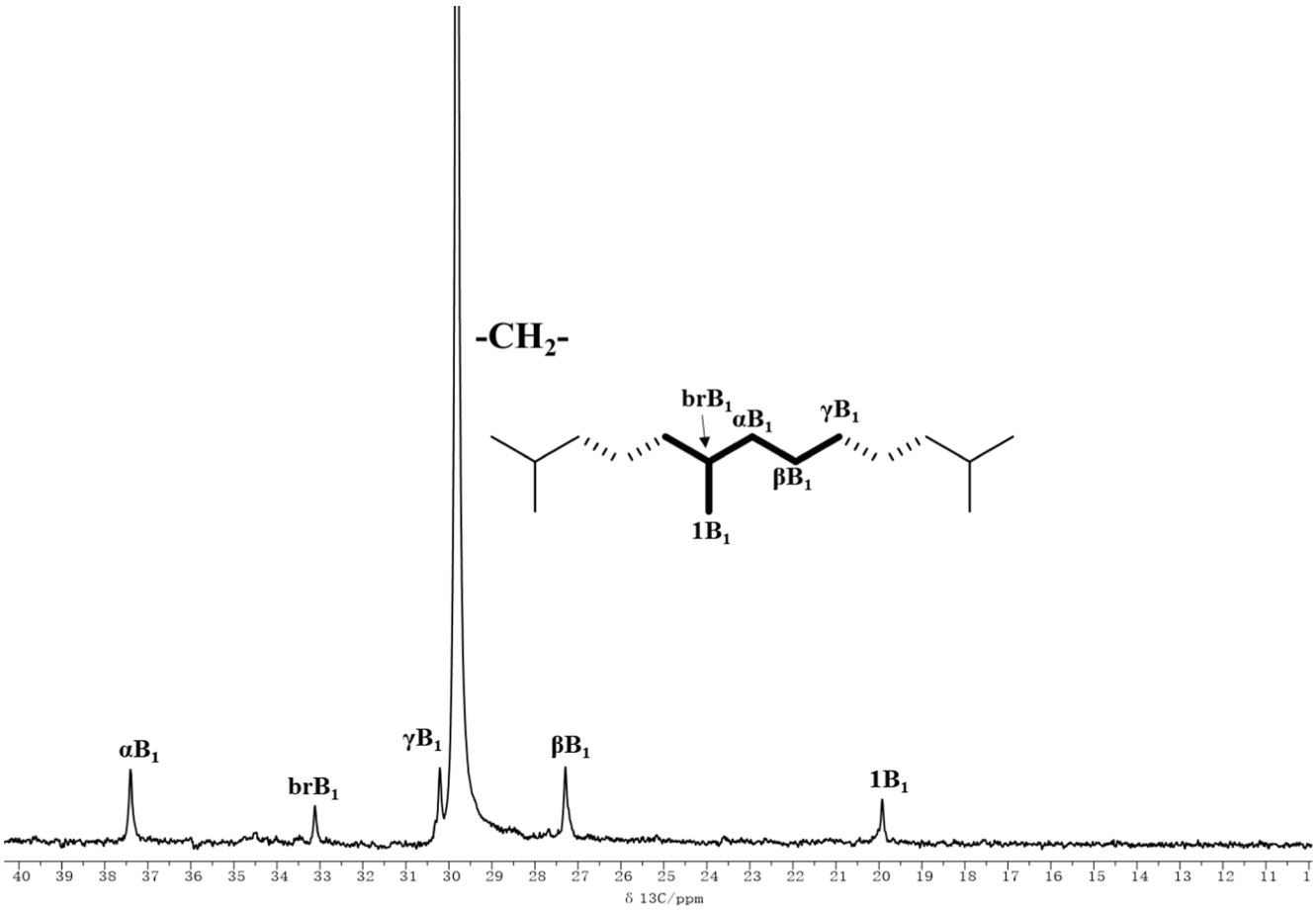

Fig. 13. High-temperature ^{13}C NMR spectra of PE sample (Entry 10, Table 2) in Bromobenzene-d_5 at 140 °C.

Table 2).

Lower catalytic activity and PE with broader polydispersity were observed for heterogeneous SACs in comparison to homogeneous polymerization (Fig. 6). Similar observations are widely reported in the literature, where the homogenous olefin catalysts were supported on the inorganic substrate for polymerization [24,25,39,40]. Besides a reduced monomer diffusion near a surface, the unexpected reduced activity and broader molecular weight distribution can be explained in terms of a higher probability of Ni center deactivation and chain termination. Such observations were reported in the literature without detailed explanation [2]. The deactivation of the Ni catalysts can be potentially attributed to the possible interactions with the supporting substrate. To substantiate this hypothesis, **Ni-FO-Al@SiO$_2$** and **Ni-FO-Si@SiO$_2$** were treated with moisture and stored under ambient air to create the hydroxyl-rich surface, giving the heterogeneous SACs as **Ni-FO-Al@SiO$_2$′** and **Ni-FO-Si@SiO$_2$′**. A significant amount of hydroxyl groups were generated on the surface either from the interaction between moisture and silica, or, the hydrolysis of Si-Cl; the corresponding chemical reactions are evidenced by the XPS analysis in Fig. 4. Meanwhile, in order to remove the influence of the extra air/moisture, both the homogenous and heterogeneous Ni catalysts were purified in argon using *Schleck* manipulations before the initiation process and ethylene polymerization. Consequently, the only difference between **Ni-FO-Si@SiO$_2$′** and **Ni-FO-Si@SiO$_2$** is the concentration of hydroxyl group on the supporting substrate. The toxicity of Si-OH moieties for the catalyst can be well explained by comparing ethylene polymerization data with **Ni-FO-Si@SiO$_2$′** (Table S3) and **Ni-FO-Si@SiO$_2$** (Table 2). Indeed, a significantly lower catalytic performance (activity and PE M_w) was observed after moisture treatment for **Ni-FO-Al@SiO$_2$′** and **Ni-FO-Si@SiO$_2$′**, as compared to **Ni-FO-Al@SiO$_2$** and **Ni-FO-Si@SiO$_2$** which were stored under an argon atmosphere (Fig. 6 and Table S3) before polymerization experiments.

As shown in Fig. 7, **Ni-FO-Si@SiO$_2$′** was selected as an example to demonstrate the surface hydroxyl deactivation mechanism during ethylene polymerization. Additional hydroxyl groups are created from the hydrolysis of Si-Cl bonds of **Ni-FO-Si@SiO$_2$′** (A) to form a hydroxyl-rich substrate (B). The hydroxyl groups on the surface are expected to quench the cocatalysts and hence down-regulate the activation of the heterogeneous SACs (C); a reduced amount of cocatalyst may still activate the heterogeneous SACs for further coordination and insertion polymerization (D). As it is well known, the cationic Ni species are responsible for the rapid chain-growth and chain-walking process. It is likely that lone paired –OH coordinates with the catalytic Ni center to generate a stable Ni-O chelate (E), because of the close distance created by the covalent tethering strategy [41]. In this way, either chain termination or catalyst deactivation can take place after the cocatalyst activation. Contrary to this, chain growth and/or chain walking can still continue without the formation of Ni-O chelate (F). This mechanism also efficiently explains why **Ni-FO-Si@SiO$_2$** and **Ni-O-Si@SiO$_2$** exhibited much lower catalytic activity than **Ni-FO-Al@SiO$_2$** and **Ni-O-Al@SiO$_2$**, which is due to the abundant presence of Cl with a lone pair. It is noted that such experimental observations are in accord with a previous work, where the immobilization of *ansa*-hafnocene complexes for propylene polymerization was related to poor catalytic performance [42].

2.4. Microstructure and morphology analysis

In ethylene homogenous polymerization, the *α*-diimine Ni complexes and the produced PE polymers were dissolved in toluene. The PE samples were precipitated in bulk and to the reactor wall when the

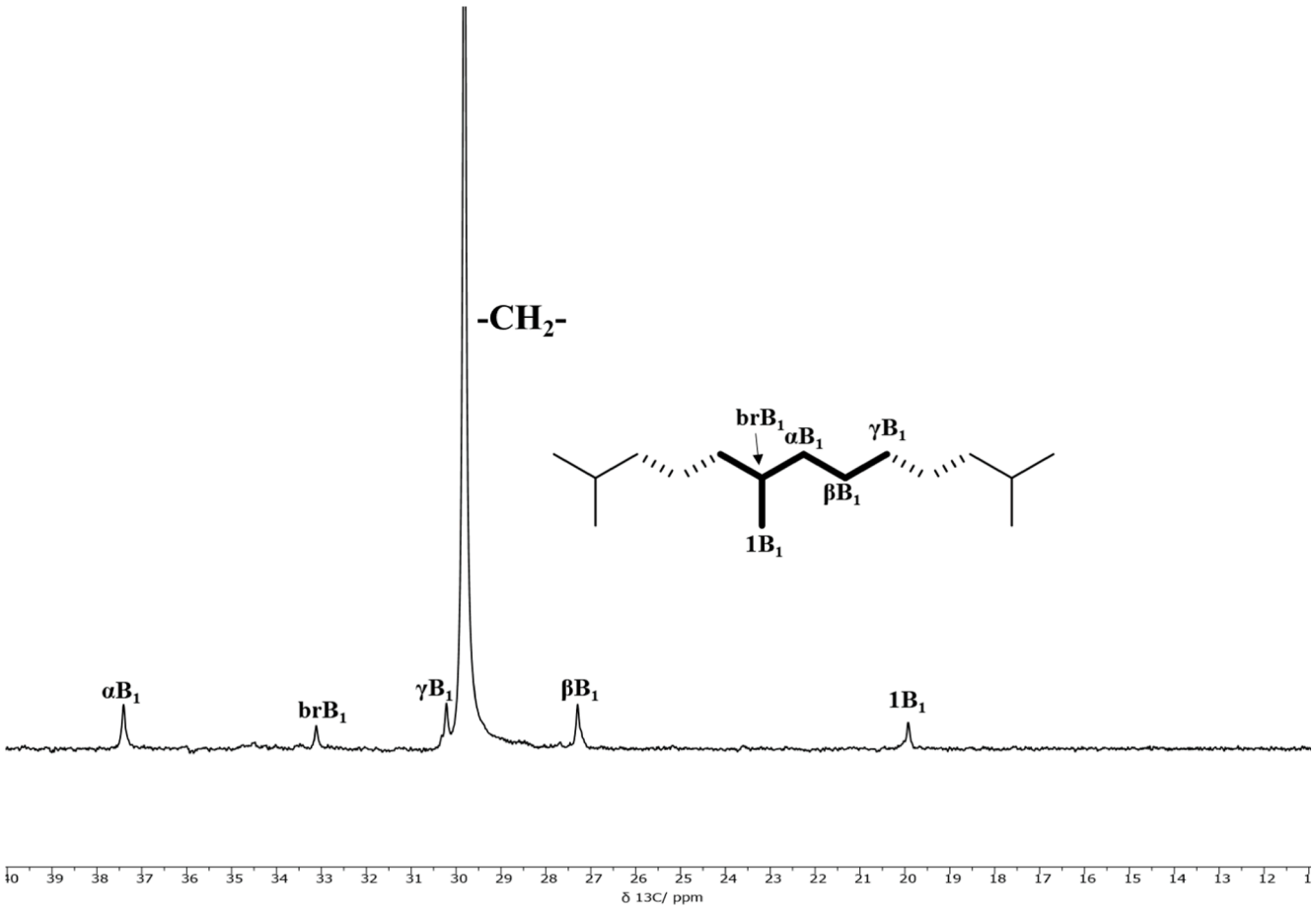

Fig. 14. High-temperature ^{13}C NMR spectra of PE sample (Entry 6, Table 2) in Bromobenzene-d_5 at 140 °C.

polymerization was terminated and quenched. This complicates the collection of the polymer and subsequent cleaning of the polymerization setup, especially in an industrial setup. Interestingly, the slurry-phase polymerization catalyzed by the supported α-diimine Ni complexes generates the polymer in a spherical shape (Fig. 8a and 8b). Such self-supporting and covalent-tethering strategies efficiently simplified the collection of the product. The polymer particles, obtained through various polymerization techniques, were characterized for their morphology using scanning electron microscopy (SEM). Interestingly, microsphere clusters and fibrous polymeric structures were observed among PE samples synthesized by heterogeneous SACs (Fig. 8c). The SEM pictures of the PE samples produced from both homogenous and self-supporting polymerization indicated uniform morphology, with only minor surface features (Fig. 8d and 8e). Furthermore, different solvents also exerted different influences on the polymer samples morphology, prepared by the heterogeneous SACs. The rope or/and cobweb-like structures on the external polymer surface were observed in toluene (Fig. 8f). Using different magnifications of the SEM images reveals the microscale and microspheric morphologies of such nascent polymer particles (Fig. 8c, 8 g, 8 h, and 8i) during the ethylene slurry-phase polymerization. In addition to normal morphology, cobweb-like fibrous structures were observed, which are most likely created from the shear forces of the stirrer. It is believed, the polymers are initially formed in the nanopores and gradually extruded out to form PE fibrous structures due to the centrifugal forces existing in the polymerization reactor.

The microstructure (branches, M_w, and T_m) of the PE samples prepared by such Ni complexes are the result of the chain-walking process, which is a competing reaction between the chain growth and chain walking in ethylene polymerization [43–45]. Catalyzed by the finely tuned complex structures and optimized polymerization techniques, this chain-walking behavior can be controlled to a certain extent [19,46,47] To further investigate the chain-walking process, high-temperature ^1H and ^{13}C NMR analysis were performed. The calculation of the PE branching density was based on the integrals of the —CH_2— and —CH_3 signals in ^1H NMR spectra, while the branching structures were distinguished by peak assignments in ^{13}C NMR spectra [11,48]. As shown in Fig. 9, a highly branched structure (up to 180.1 BD/1000C) was identified due to an accelerated chain-walking behavior at 80 °C. It is worth noting that the PE samples synthesized by the self-supported catalysts (Fig. S3 and Fig. 9a) exhibited a broader range of variation in the chain-walking process (branching densities) than the ones produced by the solution-phase catalysts (Figs. S4 and S5). Namely, in the self-supporting slurry polymerization, the chain-walking process can also be altered by the cocatalysts (Fig. S6 and Fig. 9b) and modifications of the complexes (Fig. S7 and Fig. 9c). Prominently, the PE samples produced by the covalent-tethering strategy are consistently less branched than the polymers from the self-supporting polymerization (Fig. S8 and Fig. 9d).

High-temperature ^{13}C NMR reveals significant differences between solution- and slurry-phase polymerization, even though both are catalyzed by α-diimine Ni complexes and heterogeneous SACs. There are numerous types of branches found with homogenous polymerization (both at 40 °C and 80 °C), including methyl, ethyl, propyl, butyl, amyl, and longer chains (Fig. 10 and S9). Although the slurry-phase polymerization catalyzed by the self-supported catalysts exhibited a higher rate of the chain-walking process, only methyl and propyl branches were detected with Me_2AlCl as a cocatalyst (Fig. 11 and S10). Meanwhile, the types of branches in PE samples utilizing EASC as the cocatalyst can be characterized as the methyl, ethyl, propyl, and butyl groups (Fig. 12 and S11). Obviously, a structural variation of the Ni complexes (**Ni-FOH** and

Ni-OH) did not contribute to the formation of new branching structures in the isolated PE samples. Methyl, ethyl, propyl, and butyl chains were also observed in the polymers, in the case of the **Ni-OH** system (Figure S12 and S13). Such observations clearly support the idea that the solid support must play an important role in confinement similar to steric hindrance to modulate the chain-walking behavior of Ni complexes during the ethylene monomer insertion process [16]. In support of this hypothesis, Fig. 13 shows that only the methyl group branch can be observed from the PE samples catalyzed in the slurry-phase polymerization (at 80 °C) with the covalent-tethering strategy. The same was also observed in the high-temperature ^{13}C NMR spectra of PE samples generated at 40 °C (Fig. 14). This confirms that the supporting substrate has a strong influence in controlling the chain-walking behavior of such Ni-based heterogeneous SACs. Confinement between the SiO_2 surface and the bulky *N*-aryl group provided a confined space for coordination insertion. The enhanced confinement around active Ni species restricts the chain-walking of the metal center in comparison to solution-phase polymerization. According to the current research, the modifications of the PE branching densities/types due to the modified chain-walking mechanism are dominated by the structural (electronic and steric) modifications and polymerization solution conditions such as temperature, monomer type, and pressure [2]. It confirms that surface-induced confinement is efficient to suppress branching in the chain-walking mechanism of olefin polymerization.

3. Conclusion

In a comparative study, tunable self-supporting and covalent-tethering strategies were employed to determine the catalytic performance of Ni complexes in solution and slurry-phase polymerization of ethylene. The synthesis of the heterogeneous single-atom catalysts simply involved the reaction between the applied linkers ($AlMe_3$ and $SiCl_4$) and the hydroxyl groups from both the α-diimine Ni complexes and the silica substrate. Compared to the solution-phase polymerization, a high catalytic activity of 10^6 g of PE (mol of Ni)$^{-1}$ h^{-1} and remarkable thermal stability was observed for the complexes in ethylene heterogeneous polymerization. The synthesized PEs exhibited high molecular weight (up to 10^6 g mol^{-1}) and high branching density (>100 BD/1000C). A surface hydroxyl deactivation mechanism was proposed and tested to explain the lower catalytic activity observed for the heterogeneous single-atom catalysts. The optimized slurry-phase polymerization provided an opportunity to control the polymer morphology and microstructure. Fibrous and microsphere polymers could be easily isolated that simplify the cleaning of the reactor as opposed to homogeneous polymerization. This tunability of surface-induced confinement confirms its practically relevant role for controling PE branching.

Declaration of Competing Interest

The authors declare that they have no known competing financial interests or personal relationships that could have appeared to influence the work reported in this paper.

Data availability

Data will be made available on request.

Acknowledgment

This work was financially supported by Subitex (2020-2025) and China Scholarships Council (No. 201904910562). The authors are grateful to Ms. Hania Curjel (Empa) for her kind help in English editing.

Appendix A. Supplementary material

Supplementary data to this article can be found online at https://doi.org/10.1016/j.jcat.2023.07.019.

References

[1] Z. Chen, M. Brookhart, Exploring ethylene/polar vinyl monomer copolymerizations using Ni and Pd α-diimine catalysts, Accounts Chem. Res. 51 (2018) 1831–1839.
[2] R. Wu, W.K. Wu, L. Stieglitz, S. Gaan, B. Rieger, M. Heuberger, Recent advances on α-diimine Ni and Pd complexes for catalyzed ethylene (Co) polymerization: A comprehensive review, Coordin. Chem. Rev. 474 (2023), 214844.
[3] A. Nakamura, T.M. Anselment, J. Claverie, B. Goodall, R.F. Jordan, S. Mecking, B. Rieger, A. Sen, P.W. Van Leeuwen, K. Nozaki, Ortho-phosphinobenzenesulfonate: A superb ligand for palladium-catalyzed coordination–insertion copolymerization of polar vinyl monomers, Acc. Chem. Res. 46 (2013) 1438–1449.
[4] C. Chen, Designing catalysts for olefin polymerization and copolymerization: beyond electronic and steric tuning, Nat. Rev. Chem. 2 (2018) 6–14.
[5] A. Nakamura, S. Ito, K. Nozaki, Coordination– insertion copolymerization of fundamental polar monomers, Chem. Rev. 109 (2009) 5215–5244.
[6] L.K. Johnson, C.M. Killian, M. Brookhart, New Pd (II)-and Ni (II)-based catalysts for polymerization of ethylene and. alpha.-olefins, J. Am. Chem. Soc. 117 (1995) 6414–6415.
[7] L.K. Johnson, S. Mecking, M. Brookhart, Copolymerization of ethylene and propylene with functionalized vinyl monomers by palladium (II) catalysts, J. Am. Chem. Soc. 118 (1996) 267–268.
[8] S.D. Ittel, L.K. Johnson, M. Brookhart, Late-metal catalysts for ethylene homo-and copolymerization, Chem. Rev. 100 (2000) 1169–1204.
[9] C. Tan, C. Zou, C. Chen, Material Properties of Functional Polyethylenes from Transition-Metal-Catalyzed Ethylene-Polar Monomer Copolymerization, Macromolecules 55 (2022) 1910–1922.
[10] F.-S. Liu, H.-B. Hu, Y. Xu, L.-H. Guo, S.-B. Zai, K.-M. Song, H.-Y. Gao, L. Zhang, F.-M. Zhu, Q. Wu, Thermostable α-diimine nickel (II) catalyst for ethylene polymerization: effects of the substituted backbone structure on catalytic properties and branching structure of polyethylene, Macromolecules 42 (2009) 7789–7796.
[11] D. Meinhard, M. Wegner, G. Kipiani, A. Hearley, P. Reuter, S. Fischer, O. Marti, B. Rieger, New nickel (II) diimine complexes and the control of polyethylene microstructure by catalyst design, J. Am. Chem. Soc. 129 (2007) 9182–9191.
[12] Z. Guan, P. Cotts, E. McCord, S. McLain, Chain walking: a new strategy to control polymer topology, Science 283 (1999) 2059–2062.
[13] L. Guo, S. Dai, X. Sui, C. Chen, Palladium and nickel catalyzed chain walking olefin polymerization and copolymerization, ACS Catal. 6 (2016) 428–441.
[14] Y. Zhang, Y. Zhang, X. Hu, C. Wang, Z. Jian, Advances on controlled chain walking and suppression of chain transfer in catalytic olefin polymerization, ACS Catal. 12 (2022) 14304–14320.
[15] Z. Wang, Q. Liu, G.A. Solan, W.-H. Sun, Recent advances in Ni-mediated ethylene chain growth: Nimine-donor ligand effects on catalytic activity, thermal stability and oligo-/polymer structure, Coordin Chem. Rev. 350 (2017) 68–83.
[16] J.R. Severn, J.C. Chadwick, V. Van Axel Castelli, MgCl2-based supports for the immobilization and activation of nickel diimine catalysts for polymerization of ethylene, Macromolecules 37 (2004) 6258–6259.
[17] H. Mu, G. Zhou, X. Hu, Z. Jian, Recent advances in nickel mediated copolymerization of olefin with polar monomers, Coordin. Chem. Rev. 435 (2021), 213802.
[18] M. Khoshsefat, Y. Ma, W.-H. Sun, Multinuclear late transition metal catalysts for olefin polymerization, Coordin. Chem. Rev. 434 (2021), 213788.
[19] F. Wang, C. Chen, A continuing legend: the Brookhart-type α-diimine nickel and palladium catalysts, Polym. Chem. 10 (2019) 2354–2369.
[20] K. Patel, S.H. Chikkali, S. Sivaram, Ultrahigh molecular weight polyethylene: Catalysis, structure, properties, processing and applications, Prog. Polym. Sci. 109 (2020), 101290.
[21] C. Copéret, F. Allouche, K.W. Chan, M.P. Conley, M.F. Delley, A. Fedorov, I. B. Moroz, V. Mougel, M. Pucino, K. Searles, Bridging the Gap between Industrial and Well-Defined Supported Catalysts, Angew. Chem. Int. Ed. 57 (2018) 6398–6440.
[22] J.R. Severn, J.C. Chadwick, R. Duchateau, N. Friederichs, "Bound but not gagged" immobilizing single-site α-olefin polymerization catalysts, Chem. Rev. 105 (2005) 4073–4147.
[23] H.S. Schrekker, V. Kotov, P. Preishuber-Pflugl, P. White, M. Brookhart, Efficient slurry-phase homopolymerization of ethylene to branched polyethylenes using α-diimine nickel (II) catalysts covalently linked to silica supports, Macromolecules 39 (2006) 6341–6354.
[24] C. Huang, V.A. Zakharov, N.V. Semikolenova, M.A. Matsko, Q. Mahmood, E. P. Talsi, W.-H. Sun, Comparisons between homogeneous and immobilized 1-(2, 6-dibenzhydryl-4-nitrophenylimino)-2-mesityliminoacenaphthylnickel bromide as a precatalyst in ethylene polymerization, J. Catal. 372 (2019) 103–108.
[25] C. Favero, M.B. Closs, G.B. Galland, R. Stieler, E. Rossetto, K. Bernardo-Gusmão, A binary nickel diimine-MCM-41 supported catalyst and its application in ethylene polymerization, J. Catal. 377 (2019) 63–71.
[26] F. AlObaidi, Z. Ye, S. Zhu, Ethylene Polymerization with Silica-Supported Nickel-Diimine Catalyst: Effect of Support and Polymerization Conditions on Catalyst Activity and Polymer Properties, Macromol. Chem. Phys. 204 (2003) 1653–1659.
[27] C. Favero, D. Lima, R. De Souza, K. Bernardo-Gusmão, Ethylene polymerization with a nickel diimine catalyst covalently anchored on spherical ZSM-5, New J. Chem. 41 (2017) 2333–2339.

[28] E. Kianfar, R. Azimikia, S.M. Faghih, Simple and strong dative attachment of α-diimine nickel (II) catalysts on supports for ethylene polymerization with controlled morphology, Catal. Lett. 150 (2020) 2322–2330.
[29] S. Dai, C. Chen, A Self-Supporting Strategy for Gas-Phase and Slurry-Phase Ethylene Polymerization using Late-Transition-Metal Catalysts, Angew. Chem. Int. Ed. 59 (2020) 14884–14890.
[30] R. Wu, L. Stieglitz, S. Lehner, M. Jovic, D. Rentsch, A. Neels, S. Gaan, B. Rieger, M. Heuberger, Fluorine and Hydroxyl Containing Unsymmetrical a-Diimine Ni (II) Dichlorides with Improved Catalytic Performance for Ethylene Polymerization, Eur. Polym. J. 111830 (2023).
[31] P. Rupper, M. Amberg, D. Hegemann, M. Heuberger, Optimization of mica surface hydroxylation in water vapor plasma monitored by optical emission spectroscopy, Appl. Surf. Sci. 509 (2020), 145362.
[32] J. Chastain, R.C. King Jr, Handbook of X-ray photoelectron spectroscopy, Perkin-Elmer Corporation 40 (1992) 221.
[33] L. Pei, F. Liu, H. Liao, J. Gao, L. Zhong, H. Gao, Q. Wu, Synthesis of Polyethylenes with Controlled Branching with α-Diimine Nickel Catalysts and Revisiting Formation of Long-Chain Branching, ACS Catal. 8 (2018) 1104–1113.
[34] L. Zhong, H. Zheng, C. Du, W. Du, G. Liao, C.S. Cheung, H. Gao, Thermally robust α-diimine nickel and palladium catalysts with constrained space for ethylene (co) polymerizations, J. Catal. 384 (2020) 208–217.
[35] Q. Muhammad, C. Tan, C. Chen, Concerted steric and electronic effects on α-diimine nickel-and palladium-catalyzed ethylene polymerization and copolymerization, Sci. Bull. 65 (2020) 300–307.
[36] X. Wang, L. Fan, Y. Yuan, S. Du, Y. Sun, G.A. Solan, C.-Y. Guo, W.-H. Sun, Raising the N-aryl fluoride content in unsymmetrical diaryliminoacenaphthylenes as a route to highly active nickel (II) catalysts in ethylene polymerization, Dalton Trans. 45 (2016) 18313–18323.
[37] A. Chen, D. Liao, C. Chen, Promoting Ethylene (co) Polymerization in Aliphatic Hydrocarbon Solvents Using tert-Butyl Substituted Nickel Catalysts, Chinese J Chem 40 (2022) 215–222.
[38] M.M. Stalzer, M. Delferro, T.J. Marks, Supported single-site organometallic catalysts for the synthesis of high-performance polyolefins, Catal. Lett. 145 (2015) 3–14.
[39] H. Tafazolian, D.B. Culver, M.P. Conley, A well-defined Ni (II) α-diimine catalyst supported on sulfated zirconia for polymerization catalysis, Organometallics 36 (2017) 2385–2388.
[40] J. Rodriguez, M.P. Conley, Ethylene polymerization activity of (R3P) Ni (codH)+ (cod= 1, 5-cylcooctadiene) sites supported on sulfated zirconium oxide, Inorg. Chem. 60 (2021) 6946–6949.
[41] A. Berkefeld, M. Drexler, H.M. Möller, S. Mecking, Mechanistic insights on the copolymerization of polar vinyl monomers with neutral Ni (II) catalysts, J. Am. Chem. Soc. 131 (2009) 12613–12622.
[42] M.I. Arz, T. Kratky, S. Günther, K. Rodewald, T. Burger, M. Heuberger, B. Rieger, Sequential immobilization of ansa-hafnocene complexes for propene polymerization, J. Organomet. Chem. 909 (2020), 121075.
[43] S. Mecking, L.K. Johnson, L. Wang, M. Brookhart, Mechanistic studies of the palladium-catalyzed copolymerization of ethylene and α-olefins with methyl acrylate, J. Am. Chem. Soc. 120 (1998) 888–899.
[44] C.M. Killian, D.J. Tempel, L.K. Johnson, M. Brookhart, Living polymerization of α-olefins using NiII− α-diimine catalysts. Synthesis of new block polymers based on α-olefins, J. Am. Chem. Soc. 118 (1996) 11664–11665.
[45] V.M. Möhring, G. Fink, Novel polymerization of α-olefins with the catalyst system nickel/aminobis (imino) phosphorane, Angew. Chem. Int. Ed. Eng. 24 (1985) 1001–1003.
[46] J. Xia, Y. Zhang, S. Kou, Z. Jian, A concerted double-layer steric strategy enables an ultra-highly active nickel catalyst to access ultrahigh molecular weight polyethylenes, J. Catal. 390 (2020) 30–36.
[47] S. Dai, C. Chen, Direct synthesis of functionalized high-molecular-weight polyethylene by copolymerization of ethylene with polar monomers, Angew. Chem. Int. Ed. Eng. 55 (2016) 13281–13285.
[48] R. Wu, Y. Wang, R. Zhang, C.-Y. Guo, Z. Flisak, Y. Sun, W.-H. Sun, Finely tuned nickel complexes as highly active catalysts affording branched polyethylene of high molecular weight: 1-(2, 6-Dibenzhydryl-4-methoxyphenylimino)-2-(arylimino) acenaphthylenenickel halides, Polymer 153 (2018) 574–586.